J. Biochem. **143,** 261–268 (2008)
doi:10.1093/jb/mvm217

Comparison of the Thermal Stabilities of Reverse Transcriptases from Avian Myeloblastosis Virus and Moloney Murine Leukaemia Virus

Kiyoshi Yasukawa*, Daisuke Nemoto and Kuniyo Inouye

Division of Food Science and Biotechnology, Graduate School of Agriculture, Kyoto University, Sakyo-ku, Kyoto 606-8502, Japan

Received October 21, 2007; accepted November 3, 2007; published online November 15, 2007

Reverse transcriptases (RTs) from avian myeloblastosis virus (AMV) and Moloney murine leukaemia virus (MMLV) have been most extensively used as a tool for conversion of RNA to DNA. In this study, we compared the thermal stabilities of AMV RT and MMLV RT by observing their irreversible thermal inactivation. The temperatures reducing initial activity by 50% in 10-min incubation, T_{50}, of AMV RT were 47°C without the template-primer (T/P), poly(rA)–p(dT)$_{12–18}$, and 52°C with the T/P (28 μM). T_{50} of MMLV RT were 44°C without the T/P and 47°C with the T/P (28 μM). Unexpectedly, AMV RT was considerably activated when incubated with the T/P at 45 and 48°C. Such activation was not observed in MMLV RT. These results suggest that AMV RT and MMLV RT are different in the following: (i) The intrinsic thermal stability of AMV RT is higher than that of MMLV RT; (ii) AMV RT is activated by thermal treatment with the T/P at 45–48°C; and (iii) AMV RT is stabilized by the T/P more potently than MMLV RT. Thermodynamic analysis indicates that thermal inactivation of AMV RT and MMLV RT is due to the large entropy change of activation for thermal inactivation.

Key words: avian myeloblastosis virus, Moloney murine leukaemia virus, reverse transcriptase, template-primer, thermal stability.

Abbreviations: AMV, avian myeloblastosis virus; MMLV, Moloney murine leukaemia virus; RT, reverse transcriptase; T/P, template-primer.

Reverse transcriptase (RT) is the enzyme responsible for viral genome replication, possessing RNA- and DNA-dependent DNA polymerase and RNase H activities (*1*, *2*). RTs from avian myeloblastosis virus (AMV) and Moloney murine leukaemia virus (MMLV) have been the most extensively used in cDNA synthesis (*3*) and RNA amplification reaction (*4*, *5*) due to their high catalytic activity and fidelity (*6*). AMV RT is a heterodimer consisting of 63-kDa α-subunit and 95-kDa β-subunit. The α subunit comprises the N-terminal polymerase and the C-terminal RNase H domains, and the β subunit comprises these two domains and the C-terminal integrase domain. MMLV RT is a 75-kDa monomer comprising the same domains as the α subunit of AMV RT. The active sites for DNA polymerase and RNase H activities of RT are different and functionally uncoupled (*7*). Recombinant MMLV RT has been expressed in soluble fractions in *Escherichia coli*, from which sufficient amounts of active enzymes have been purified (*8–10*). In contrast, recombinant AMV RT has barely been expressed in soluble fractions in *E. coli* (*11*). Recently, active recombinant AMV RT was expressed in insect cells (*12*). The three-dimensional structure of MMLV RT is known (*13–15*), but that of AMV RT is not.

In cDNA synthesis and RNA amplification, elevated reaction temperature has been highly desired because it reduces RNA secondary structure and non-specific binding of primer. Thermal stability of RT has been markedly improved by eliminating its RNase H activity (*16*). As a result, reaction temperature of RT for reverse transcription has increased from 37–45°C to 50–60°C (*17*). However, RNase H-minus RT cannot be used in RNA amplification reaction because it requires both DNA polymerase and RNase H activities. Therefore, RNA amplification reaction has been performed at low temperatures such as 41–43°C (*4*, *5*, *18*, *19*). In addition, RNA is stable at 65°C, and thus further stabilization of RT should be desirable for DNA polymerase reaction. The improvement in the thermal stabilities of AMV RT and MMLV RT is still an important subject for their wide-range practical use.

It is thought that AMV RT is more thermally stable than MMLV RT because the reaction with AMV RT has been performed in most of the cases at higher temperature by 3–5°C than that with MMLV RT (*20*). However, little is known about their thermal stabilities. In this study, we compare the thermal stabilities of AMV RT and MMLV RT by observing their irreversible thermal inactivation, and demonstrate that AMV RT has higher intrinsic thermal stability and is more potently stabilized by the template-primer than MMLV RT.

*To whom correspondence should be addressed. Tel: +81-75-753-6267, Fax: +81-75-753-6265,
E-mail: yasukawa@kais.kyoto-u.ac.jp

MATERIALS AND METHODS

Materials—Native AMV RT (Lot LS02207-7) purified from AMV was purchased from Life Sciences, Inc (Petersburg, FL). Poly(rA)–p(dT)$_{12–18}$ (Lot HA0166), dTTP (Lot 340755), and [methyl-^{3}H]dTTP (1.52 TBq/mmol) (Lot 209) were purchased from GE Healthcare (Buckinghamshire, UK). The glass filter GF/C 2.5 cm is a product of Whatman (Middlesex, UK). RT concentration was determined according to the method of Bradford (*21*) using Protein Assay CBB Solution (Nacalai Tesque, Kyoto) with bovine serum albumin (Lot M3G9751, Nacalai Tesque) as a standard.

Expression and Purification of MMLV RT—A pUC19 plasmid that contains the complete MMLV gene (8332 bp) was used as a template for PCR. The 1984-bp fragment containing the MMLV RT gene was amplified using the following nucleotide primers: 5′-TCCATA TGACATGGCTGTCTGATTTTCCTC3-3′ and 5′-CTGAAT TCTTAGAGGAGGGTAGAGGTGTCT-3′. The amplified DNA product was digested with the restriction enzymes *Nde*I and *Eco*RI and inserted in pET-22b(+) (Merck Bioscience, Tokyo) digested with *Nde*I and *Eco*RI to produce pET-MRT. BL21(DE3) [F^-, *ompT*, *hsdS*$_B$ (r_B^- m_B^-) *gal dcm* (DE3)] cells were transformed with pET-MRT. The overnight culture of the transformant (1 ml) was added to 100 ml of L broth containing 50 μg/ml ampicillin and incubated with shaking at 37°C. When OD_{660} reached 0.6–0.8, IPTG (0.1 ml of 0.5 M) was added, and growth was continued for 4 h. The cells were harvested by centrifugation at 10,000*g* for 10 min, suspended with 10 ml of 50 mM sodium phosphate (pH 7.8), 5% glycerol, 300 mM NaCl, 0.4% Triton X-100, 1 mM PMSF and disrupted by sonication. The supernatant was collected by centrifugation at 10,000*g* for 10 min, to which polyethyleneimine [0.1 ml of 25%(w/v)] was added. The pellet resulted was removed by centrifugation at 10,000*g* for 10 min, and solid $(NH_4)_2SO_4$ was added to the supernatant to be 40% saturation. The pellet resulted was collected by centrifugation at 10,000*g* for 10 min, dissolved in 1 ml of 20 mM potassium phosphate (pH 7.2), 2 mM DTT, 0.2% Triton X-100, 50% glycerol and dialysed against the same buffer. MMLV RT thus purified was stored at –80°C before use.

SDS–PAGE—SDS–PAGE was performed in a 10% polyacrylamide gel under reducing conditions according to the method of Laemmli (*22*). Proteins were reduced by treatment with 2.5% of 2-mercaptoethanol at 100°C for 10 min, and then applied onto the gel. A constant current of 40 mA was applied for 40 min. After electrophoresis, proteins were stained with Coomassie Brilliant Blue R-250. The molecular mass marker kit consisting of myosin (200 kDa), β-galactosidase (116 kDa), bovine serum albumin (66.3 kDa), rabbit muscle aldolase (42.4 kDa) and bovine erythrocyte carbonic anhydrase (30.0 kDa) was a product of Daiichi Pure Chemicals (Tokyo).

Reverse Transcription Assay—RT activity was determined by measuring the incorporation of [^{3}H]dTTP to poly(rA)–p(dT)$_{12–18}$. Unless described otherwise, reaction was carried out in 25 mM Tris–HCl (pH 8.3), 50 mM KCl, 2 mM DTT, 5 mM $MgCl_2$, 25 μM poly(rA)–p(dT)$_{12–18}$ (the concentration is expressed as that of p(dT)$_{12–18}$), 0.4 mM [^{3}H]dTTP (3.7 MBq/ml; 1.85 Bq/pmol) and 5 nM RT at 37°C. Aliquot (20 μl) was taken from the reaction mixture at specified time and immediately spotted onto the glass filter. Unincorporated [^{3}H]dTTP was removed by three washes of chilled 5%(w/v) trichloroacetic acid for 10 min each followed by one wash of chilled 95% ethanol. The radioactivity of the dried filters were counted in 3 ml of toluene containing 4 g/l diphenyloxazol and 0.1 g/l 1,4-bis-2-(5-phenyloxazolyl) benzene. The reaction rate was estimated by the time-course of the amounts of [^{3}H]dTTP incorporated. The kinetic parameters, k_{cat} and K_m, were determined based on the Michaelis–Menten equation using the non-linear least-squares methods (*23*) with Kaleida Graph Version 3.5 (Synergy Software, Essex, VT).

Irreversible Thermal Inactivation of RT—RT (100 nM) in 10 mM potassium phosphate (pH 7.6), 2 mM DTT, 0.2%(v/v) Triton X-100, 10%(v/v) glycerol was incubated in the presence or absence of 28 μM poly(rA)–p(dT)$_{12–18}$ at different temperatures for specified time followed by the incubation on ice for 30–60 min. The remaining activity of the RT toward reverse transcription was determined at 37°C as described before.

Thermodynamic Analysis of Irreversible Thermal Inactivation of RT—Assuming that the thermal inactivation reaction of RT is irreversible and consists of only one step, the first-order rate constant, k_{obs}, of the thermal inactivation was evaluated by plotting logarithmic values of the residual activity against the time of heat treatment according to Eq. 1.

$$\ln B = A - k_{obs}\, t \tag{1}$$

where A is the constant term, and B is the relative activity (%) defined as the ratio of the initial reaction rate at a time for the thermal incubation (=t) to that without the incubation. The activation energy, E_a, for the thermal inactivation was determined from an Arrhenius plot according to Eq. 2, and the Gibbs free energy change of activation, $\Delta G^{\ddagger}$, for the thermal inactivation was determined according to Eq. 3 (*24*).

$$\ln(k_{obs}) = A - \left(\frac{E_a}{R}\right)\left(\frac{1}{T}\right) \tag{2}$$

$$\Delta G^{\ddagger} = -RT\left[\ln(k_{obs}) - \ln\left(\frac{RT}{Nh}\right)\right] \tag{3}$$

where A, R, T, N and h are the constant term, the gas constant (=8.314 J K^{-1} mol^{-1}), absolute temperature in degrees Kelvin, Avogadro number (=6.022×10^{23} mol^{-1}), and Plank constant (=6.626×10^{-34} J s), respectively. The enthalpy change of activation, $\Delta H^{\ddagger}$, for the thermal inactivation was estimated according to Eq. 4. Using estimated $\Delta G^{\ddagger}$ and $\Delta H^{\ddagger}$ values at a certain temperature, the entropy change of activation, $\Delta S^{\ddagger}$, for the thermal inactivation was estimated according to Eq. 5.

$$\Delta H^{\ddagger} = E_a - RT \tag{4}$$

$$\Delta S^{\ddagger} = \left(\frac{\Delta H^{\ddagger} - \Delta G^{\ddagger}}{T}\right) \tag{5}$$

The temperature required to reduce initial activity by 50% in 10-min incubation, T_{50}, was estimated by

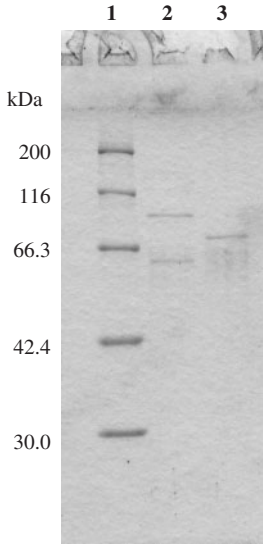

Fig. 1. **SDS–PAGE of RT under reducing condition.** Lane 1, molecular-mass marker; lane 2, AMV RT (220 ng); lane 3, MMLV RT (220 ng).

Arrhenius plot as the temperature at which the k_{obs} value gives the remaining activity of 50% at 10 min according to Eq. 1.

RESULTS

Kinetic Analysis of Reverse Transcription Reaction of RT—In this study, we used native AMV RT purified from AMV and recombinant MMLV RT expressed in *E. coli*. Upon SDS–PAGE under reducing condition, AMV RT yielded two bands with a molecular mass of 95 and 63 kDa, and MMLV RT yielded a single band with a molecular mass of 75 kDa (Fig. 1).

The reaction rates for reverse transcription at various dTTP concentrations (0–400 μM) with 5 nM RT at 37°C are shown in Fig. 2. A saturated profile of the Michaelis–Menten kinetics was obtained, and the K_m and k_{cat} values were separately determined (Table 1). Both K_m and k_{cat} values of MMLV RT were 4-fold higher than those of AMV RT, and their k_{cat}/K_m values are almost the same.

In general, one unit of RT is defined as the amount which incorporates 1 nmol of dTTP into poly(rA)–p(dT)$_{12–18}$ in 10 min at 37°C. According to Table 1 and the Michaelis–Menten equation, expressed as $v = k_{cat}[E]_o[S]_o/(K_m + [S]_o)$, where v, $[E]_o$ and $[S]_o$ mean the reaction rate, the initial enzyme concentration (= 5 nM) and the initial substrate concentration (= 500 μM), respectively, the reaction rates of AMV RT and MMLV RT are calculated to be 37 and 110 nM s^{-1}, respectively. Based on the molecular mass of 158 kDa for AMV RT and 75 kDa for MMLV RT, their specific activities are calculated to be 2.8×10^4 and 1.8×10^5 units/mg, respectively. These values are similar to the specific activities of AMV RT (3.6×10^4 units/mg) (supplier's information and our protein quantification) and MMLV RT (2.3×10^5 units/mg) (*16*), respectively, as assessed by the incorporation of dTTP into poly(rA)–p(dT)$_{12–18}$ with the dTTP concentration of 500 μM.

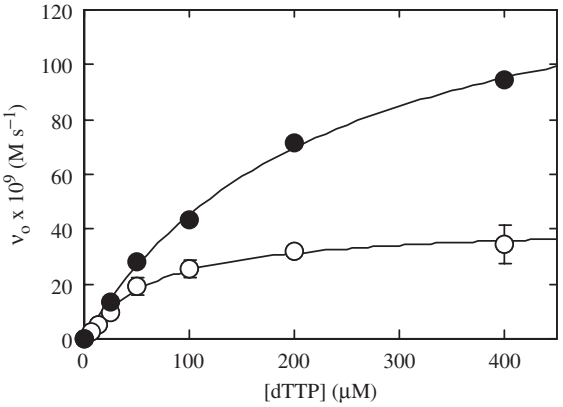

Fig. 2. **Dependence on the substrate concentration of the initial reaction rate of RT-catalyzed reverse transcription.** The reaction was carried out with AMV RT (open circle) and MMLV RT (filled circle) at 5 nM, at 37°C. The concentration of poly(rA)–p(dT)$_{12–18}$ was 25 μM. Error bars indicate SD values. Solid line represents the best fit of the Michaelis–Menten equation.

Table 1. **Kinetic parameters of RT in the reverse transcription reaction at 37°C.**

	K_m (μM)	k_{cat} (s^{-1})	k_{cat}/K_m (μM^{-1} s^{-1})
AMV RT	67.2 ± 8.5	8.3 ± 0.4	0.12 ± 0.01
MMLV RT	232 ± 19	33 ± 1	0.14 ± 0.01

The average of triplicate determination with SD value is shown.

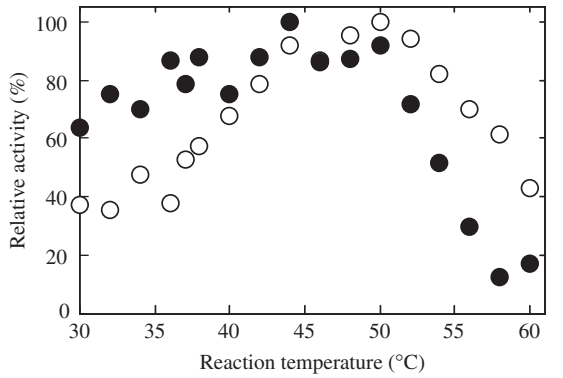

Fig. 3. **Dependence on temperature of the initial reaction rate of RT-catalyzed reverse transcription.** The reaction was carried out with AMV RT (open circle) and MMLV RT (filled circle) at 5 nM. The concentrations of poly(rA)–p(dT)$_{12–18}$ and [^{3}H]dTTP were 25 μM and 0.4 mM, respectively. The relative activity is defined as the ratio of the initial reaction rate at the indicated temperature to that at the optimal temperature (100×10^{-9} M s^{-1} at 50°C for AMV RT and 121×10^{-9} M s^{-1} at 44°C for MMLV RT).

Optimal Reaction Temperature of RT—We next examined the optimal reaction temperature of AMV RT and MMLV RT. The reverse transcription activities at various temperatures ranging 30–60°C are shown in Fig. 3. The plot showed a curve with the optimal temperature range of around 44–50°C for AMV RT and MMLV RT. However, the relative activity of MMLV RT decreased more sharply than that of AMV RT with

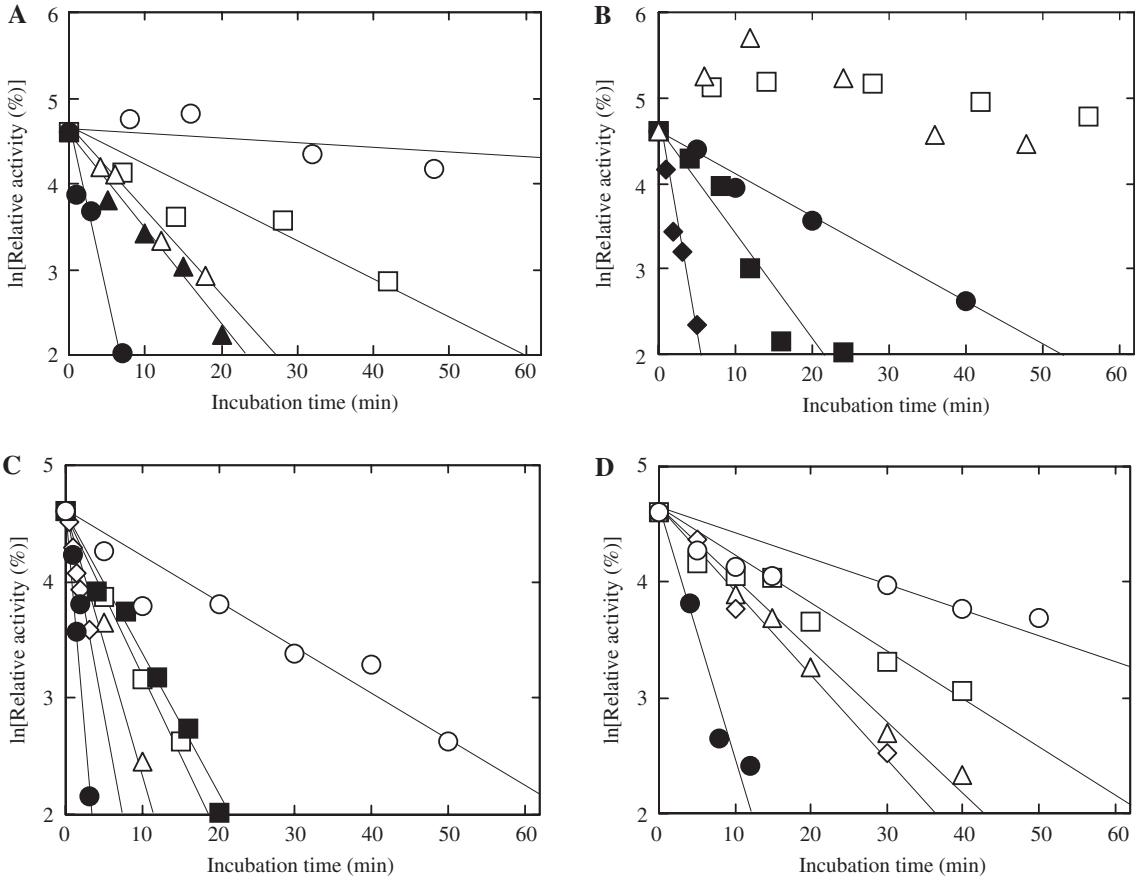

Fig. 4. **Thermal inactivation of RT.** The reverse transcription reaction was carried out with RT at 5 nM, respectively. The relative activity is defined as the ratio of the initial reaction rate with the incubation for the indicated time to that without the incubation (31×10^{-9} M s^{-1} for AMV RT and 60×10^{-9} M s^{-1} for MMLV RT). (A) Thermal treatment of AMV RT in the absence of poly(rA)–$p(dT)_{12–18}$. Thermal treatment was carried out at 42 (open circle), 45 (open square), 48 (open triangle, filled triangle), and 50°C (filled circle) with RT at 100 (open circle, open square, open triangle, filled circle) and 500 nM (filled triangle). The natural logarithm of the initial reaction rate was plotted against the incubation time. The first-order rate constant of thermal inactivation of RT, k_{obs}, was estimated from the slope. k_{obs} at 42 (open circle), 45 (open square), 48 (open triangle), 48 (filled triangle) and 50°C (filled circle) were determined to be 1.6×10^{-4}, 7.1×10^{-4}, 1.6×10^{-3}, 1.8×10^{-3} and 5.7×10^{-3} s^{-1}, respectively. (B) Thermal treatment of AMV RT in the presence of poly(rA)–$p(dT)_{12–18}$. Thermal treatment was carried out with RT at 100 nM. k_{obs} at 50 (filled circle), 52 (filled square) and 55°C (filled diamond) were determined to be 8.4×10^{-4}, 2.0×10^{-3} and 7.8×10^{-3} s^{-1}, respectively. k_{obs} at 45 (open square) and 48°C (open triangle) were not obtained. (C) Thermal treatment of MMLV RT in the absence of poly(rA)–$p(dT)_{12–18}$. Thermal treatment was carried out at 42 (open circle), 44 (open square, filled square), 46 (open triangle), 48 (open diamond) and 50°C (filled circle) with RT at 100 (open circle, open square, open triangle, open diamond, filled circle) and 500 nM (filled square). k_{obs} at 42 (open circle), 44 (open square), 44 (filled square), 46 (open triangle), 48 (open diamond) and 50°C (filled circle) were determined to be 6.4×10^{-4}, 2.2×10^{-3}, 2.0×10^{-3}, 3.5×10^{-3}, 5.6×10^{-3} and 1.1×10^{-2} s^{-1}, respectively. (D) Thermal treatment of MMLV RT in the presence of poly(rA)–$p(dT)_{12–18}$. Thermal treatment was carried out with RT at 100 nM. k_{obs} at 42 (open circle), 44 (open square), 46 (open triangle), 48 (open diamond) and 50 °C (filled circle) were determined to be 3.5×10^{-4}, 6.9×10^{-4}, 1.0×10^{-3}, 1.2×10^{-3} and 3.2×10^{-3} s^{-1}, respectively.

increasing temperature from 52 to 60°C. In contrast, the relative activity of MMLV RT was higher than that of AMV at lower temperatures than 40°C.

Irreversible Thermal Inactivation of RT

Figure 4 shows the remaining reverse transcription activity of RT at 37°C after heat treatment at 42–55°C in the absence or presence of the T/P, poly(rA)–$p(dT)_{12–18}$. Unexpectedly, the AMV RT activity increased considerably by the incubation in the presence of the T/P at 45 and 48°C for all the times measured (Fig. 4B). The maximum activity was 300% of the initial activity when AMV RT was incubated at 48°C for 12 min in the presence of the T/P. Such activation was not observed when AMV RT was incubated at 42–50°C in the absence of the T/P (Fig. 4A) and at 50–55°C in the presence of the T/P (Fig. 4B). MMLV RT was not activated whether it was incubated in the absence or presence of the T/P (Fig. 4C and D). Except for heat treatment of AMV RT at 45 and 48°C in the presence of the T/P, linear relationships between the natural logarithm of the remaining activity against the incubation time were obtained at all temperatures. The inactivation curve of AMV RT treated at 48°C with the concentration of 500 nM was almost the same as that with the concentration of 100 nM (Fig. 4A). Similar result was obtained for MMLV RT that received heat treatment at 44°C (Fig. 4C), suggesting that the inactivation reaction is independent of RT concentration. Therefore, the thermal inactivation could be regarded as a first-order reaction.

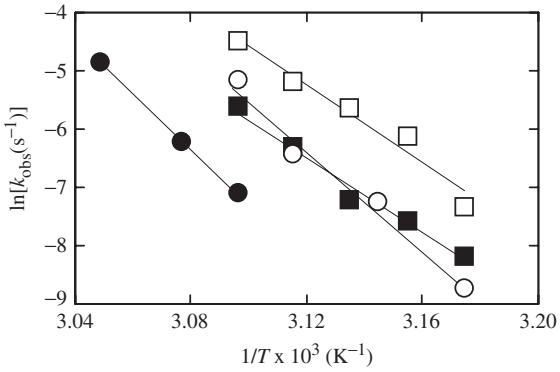

Fig. 5. **Arrhenius plot of k_{obs} values of AMV RT and MMLV RT.** The natural logarithm of k_{obs} was plotted against the reciprocal of the absolute temperature. Activation energy, E_a, was calculated from the slope: AMV RT incubated without poly(rA)–p(dT)$_{12–18}$ (open circle), 358 ± 36 kJ mol^{-1}; AMV RT incubated with poly(rA)–p(dT)$_{12–18}$ (filled circle), 393 ± 8 kJ mol^{-1}; MMLV RT incubated without poly(rA)–p(dT)$_{12–18}$ (open square), $280 \text{ kJ} \pm 33$ mol^{-1}; MMLV RT incubated with poly(rA)–p(dT)$_{12–18}$ (filled square), 272 ± 22 kJ mol^{-1}.

Table 2. **Thermodynamic parameters for thermal inactivation of RT.**

	Template-primer	*Ea* (kJ mol^{-1})	$\Delta G^{\ddagger}$ (kJ mol^{-1})	$\Delta H^{\ddagger}$ (kJ mol^{-1})	$\Delta S^{\ddagger}$ (J mol^{-1} K^{-1})
AMV RT	minus	358 ± 36	91 ± 0	355 ± 36	819 ± 112
AMV RT	plus	393 ± 8	94 ± 0	390 ± 8	917 ± 24
MMLV RT	minus	280 ± 33	87 ± 0	278 ± 33	589 ± 101
MMLV RT	plus	272 ± 22	90 ± 0	269 ± 22	553 ± 42

Ea is the activation energy. $\Delta G^{\ddagger}$, $\Delta H^{\ddagger}$, and $\Delta S^{\ddagger}$ are the Gibbs free energy change of activation, the enthalpy change of activation, and the entropy change of activation, respectively, at 50°C.

Figure 5 shows Arrhenius plot of the first-order rate constant, k_{obs}, of the thermal inactivation of RT. Linear relationship was held between the natural logarithm of k_{obs} and 1/T. We estimated the temperatures required to reduce initial activity by 50% in 10-min incubation, T_{50}, from Arrhenius plot as described in the section of MATERIALS AND METHODS. In the absence of the T/P, T_{50} of AMV RT and MMLV RT were 47 and 44°C, respectively, demonstrating that the intrinsic stability of AMV RT was higher than that of MMLV RT by 3°C in T_{50}. In the presence of the T/P (28 μM), T_{50} of AMV RT and MMLV RT increased to 52 and 47°C, respectively, demonstrating that the stabilizing effect of the TP on AMV RT was more potent than that on MMLV RT by 2°C in the increment of T_{50} by the addition of the T/P.

Table 2 shows the thermodynamic parameters for irreversible thermal inactivation of RT. In the absence of the T/P, the large $\Delta H^{\ddagger}$ values of AMV RT and MMLV RT (355 ± 36 and 278 ± 33 kJ mol^{-1}, respectively) are compensated by large values (819 ± 112 and 589 ± 101 J mol^{-1} K^{-1}, respectively) of $\Delta S^{\ddagger}$, resulting in small values (91 ± 0 and 87 ± 0 kJ mol^{-1}, respectively) of $\Delta G^{\ddagger}$. This suggests that thermal inactivation of intrinsic AMV RT and MMLV RT was due to the large entropy change of activation for thermal inactivation. Such enthalpy–entropy compensation was also observed in the presence of the T/P. In addition, there is a future that in the presence of the T/P, the AMV RT has 10%-increased $\Delta H^{\ddagger}$ and 12%-increased $\Delta S^{\ddagger}$ values while MMLV RT has 3%-decreased $\Delta H^{\ddagger}$ and 6%-decreased $\Delta S^{\ddagger}$ values compared to those in its absence, suggesting the difference between the stabilizing mechanisms of the T/P on AMV RT and MMLV RT.

DISCUSSION

Thermal Stability of Intrinsic RT and the Stabilizing Effect of the T/P on RT—In this study, we examined irreversible thermal inactivation of RT and found that AMV RT was more thermally stable and stabilized by the T/P more effectively than MMLV RT. It should be noted that the observed irreversible thermal inactivation of RT in the presence of the T/P at the respective temperatures should be the combination of the inactivation of the free RT and that of the T/P-bound RT. Dissociation constants of RTs to the T/P at certain temperatures have been reported (*25–27*), but their temperature-dependences have not been known.

Gerard *et al*. (*25*) reported that AMV RT was less thermally stable than MMLV RT and that AMV RT was stabilized by the T/P (100 nM) while MMLV RT was not. We observed higher thermal stability of AMV RT than that of MMLV RT at temperatures range of 42–50°C (Fig. 4). More specifically, from the first-order rate constant, k_{obs}, of the thermal inactivation of RT, the half-lives at 50°C of AMV RT and MMLV RT (100 nM) in the absence of the T/P were calculated to be 3.6 and 1.0 min, and those in its presence (28 μM) were calculated to be 14 and 3.1 min. In the report by Gerard *et al*. (*25*), the half-lives at 50°C of AMV RT and MMLV RT (40–80 nM) in the absence of the T/P were 1.6 and 2.8 min, and those in its presence (200 nM) were 15 and 2.5 min. The reason for the opposite order of the half-lives at 50°C of AMV RT and MMLV RT in the absence of the T/P is not known. On the other hand, the discrepancy in the stabilizing effects of the T/P on irreversible thermal inactivation of MMLV RT might be merely the difference in the T/P concentration during thermal treatment [28 μM in this study and 200 nM in the study by Gerard *et al*. (*25*)], considering that enzymes are generally stabilized by binding to substrate (*26*). Dissociation constant of MMLV RT to the T/P was 29 nM at 23°C (*25*), which is around 30-fold higher than those of AMV RT (1.2 nM at 23°C) (*25*) and HIV-1 RT (<1 nM at 25°C) (*27*), suggesting that high concentration TP is required to stabilize MMLV RT.

Dependence on temperature of the reaction rate of RT-catalysed reverse transcription revealed that the relative activity of AMV RT was significantly higher than that of MMLV RT at 52–60°C (Fig. 3). This might be explained by the observation in the irreversible thermal inactivation that AMV RT is considerably more stable than MMLV RT at temperatures higher than 50°C in the presence of the T/P (Fig. 4B and D).

Comparison of the Thermal Stabilities of AMV RT and MMLV RT with those of Other Proteins—Arrhenius plot

of k_{obs} values (Fig. 5) revealed that the E_a values of AMV RT and MMLV RT for irreversible thermal inactivation are large [(358 ± 36) and (280 ± 33) kJ mol^{-1}, respectively] (Table 2) despite their low T_{50} (temperatures giving 50% inactivation in 10-min incubation) of 47 and 44°C, respectively. This characteristic of AMV RT and MMLV RT becomes obvious by comparison with other proteins. For example, the E_a value and T_{50} are 237 kJ mol^{-1} and 69°C for human matrix metalloproteinase 7 (*28*), and 268 kJ mol^{-1} and 77°C for bovine erythrocyte Cu,Zn-superoxide dismutase (*29*), respectively. In addition, the E_a value and T_{50} (temperatures giving 50% inactivation in 30-min incubation) are 249 kJ mol^{-1} and 75°C for *Bacillus amyloliquefaciens* α-amylase (BAA) in the presence of Ca^{2+} ion, 124 kJ mol^{-1} and 44–45°C for BAA in its absence (*30*), and 87 kJ mol^{-1} and 88°C for 0.19 α-amylase inhibitor from wheat kernel (0.19AI) (*31*). As the result of high E_a and low $\Delta G^{\ddagger}$ values of AMV RT and MMLV RT, their calculated $\Delta S^{\ddagger}$ values are markedly large [(819 ± 112) and (589 ± 101) J mol^{-1} K^{-1}, respectively] compared to, for example, those of BAA in the presence of Ca^{2+} ion (406 J mol^{-1} K^{-1}), BAA in its absence (77 J mol^{-1} K^{-1}) (*30*), and 0.19AI (–78.8 J mol^{-1} K^{-1}) (*31*). In other words, thermal denaturation of RT is driven by the large entropy change of activation for thermal inactivation. The N-terminal polymerase domains of AMV RT, MMLV RT and HIV-1 RT contain common five domains; fingers, palm, thumb, connection and RNase H (*14*), suggesting that RT is evolved to have such an elaborate structure and elicit high catalytic activity at the cost of the thermal stability.

It is well known that there is a compromise between activity and stability in various enzymes (*28*, *32–34*). Active-site mutations which increase protein stability are in most of the cases accompanied with decrease in enzyme activity. However, the results with thermolysin (*35*) and thermolysin-like protease (*36*) have shown that when thermal stability of an enzyme is governed by a local unfolding far from the active site, the stability might be improved by site-directed mutagenesis without affecting the activity. Thermal stability of RT has been markedly improved by eliminating its RNase H activity (*16*), suggesting that the active site for RNase H activity might be responsible for unfolding of the whole RT.

Conformation of the T/P-AMV RT complex—According to the previous reports on the structural study of HIV-1 RT, a heterodimer consisting of 51-kDa α subunit (p51) and 66-kDa β subunit (p66), (*37*, *38*), the tip of the p66 thumb domain interacts with the p66 fingers domain in the absence of the T/P, and the cleft is 15 Å in diameter, which is large enough to accommodate a single-stranded but not a double-stranded DNA. When the T/P is bound in the cleft, the tip of the p66 thumb domain moves 25–30 Å away from the p66 fingers domain to expand the cleft. We presume that similar conformational change occurs in heterodimeric AMV RT, but not in monomeric MMLV RT. Site-directed mutagenesis study and/or crystallographic analysis is required to clarify the conformational change of AMV RT by the T/P binding. Establishment of an expression system for recombinant AMV RT is currently underway.

Insights into the Activation of AMV RT by the Thermal Treatment in the Presence of the T/P—The reaction rate of AMV RT increased by 3-fold at the maximum by the thermal treatment at 48°C in the presence of the T/P (Fig. 4B). As described in the section of MATERIALS AND METHODS, AMV RT was incubated on ice for 30–60 min after thermal treatment and then subjected to the reaction at 37°C. Therefore, the activation is apparently irreversible. To our knowledge, such activation has not been reported in HIV-1 RT.

In general, thermal inactivation of AMV RT can be interpreted according to the simple two-state model as expressed by Scheme 1 where N and U represent the native and unfolded AMV RT species, respectively. However, AMV RT was activated when incubated with the T/P at 45 or 48°C (Fig. 4B). The activity reached the maximum at around 10 min and then decreased gradually. This implies that the denaturation model of AMV RT in the presence of the T/P should be improved by considering the presence of the intermediate (I) with improved activity as expressed by Scheme 2.

$$N \rightarrow U \qquad \text{Scheme 1}$$

$$N \rightarrow I \rightarrow U \qquad \text{Scheme 2}$$

It should be mentioned that based on Scheme 2, the remaining reverse transcription activity of AMV RT should drop from the relative activity higher than 100% with increasing incubation time, but such activation was not observed at 50–55°C (Fig. 4B). In addition, considering that the T/P binds MMLV RT more weakly than AMV RT, the possibility cannot be denied that the denaturation model of MMLV RT in the presence of the T/P is also expressed by Scheme 2. In regard of this, the activation of MMLV RT by the thermal treatment in the presence of the T/P was not observed (Fig. 4D), and the T/P-mediated stabilization of AMV RT is driven by the increase in the $\Delta H^{\ddagger}$ value while that of MMLV RT is driven by the decrease in the $\Delta S^{\ddagger}$ value (Table 2). We thus speculate that the stabilizing mechanisms of the T/P on AMV RT and MMLV RT are different.

The time-dependence of the reverse transcription activity of AMV RT after heat treatment in the presence of the T/P is the next subject. In addition, it should be determined whether the activation is induced by the decrease in K_m and/or the increase in k_{cat}. Regarding the activation-and-inhibition dual effect of thermal treatment on RT, we have reported similar effect of alcohols on neuraminidase (*39*) and that of cobalt ion on thermolysin (*40*, *41*). In both cases, there are two types of binding site in enzyme, one for the activation and the other for inhibition, and the effects are reversible.

Kinetic Parameters of Reverse Transcription Reaction of RT—The K_m and k_{cat} values of AMV RT (Table 1) are almost the same as those previously reported (*42*) while those of MMLV RT are around 10-fold higher than the ones previously reported (*43*, *44*). Generally, the reaction rate of RT strictly depends on the T/P, e.g. the nucleotide lengths of the template and the primer, the template/primer molar ratio, and their sequence. For example, displacement synthesis is 3–4-fold slower than non-displacement synthesis in MMLV RT (*45*). The reaction rate is different between poly(rA)–p(dT) and

poly(rC)–p(dG) (*42*, *46*). Therefore, the reason of the discrepancy is difficult to be estimated. However, it seems reasonable that the k_{cat} value of MMLV RT is higher than that of AMV RT, considering that the specific activity, which is measured under the condition where the concentration of dTTP (500 μM) is higher than K_m, of MMLV RT is higher than that of AMV RT (*16*).

In conclusion, AMV RT is more thermally stable than MMLV RT whether the T/P is absent or present. The elucidation of the mechanisms of the stabilization by the T/P and the activation by thermal treatment in the presence of the T/P will provide the strategy to generate RT with improved stability by site-directed mutagenesis without diminishing its activity.

This study was supported in part (K.Y.) by Grants-in-Aid for Scientific Research (No. 19580104) from the Japan Society of the Promotion of Sciences.

REFERENCES

1. Temin, H.M. and Mizutani, S. (1970) RNA-dependent DNA polymerase in virions of Rous sarcoma virus. *Nature* **226**, 1211–1213
2. Baltimore, D. (1970) RNA-dependent DNA polymerase in virions of RNA tumour viruses. *Nature* **226**, 1209–1211
3. Kimmel, A.R. and Berger, S.L. (1987) Preparation of cDNA and the generation of cDNA libraries: overview. *Methods Enzymol.* **152**, 307–316
4. Kievits, T., van Gemen, B., van Strijp, D., Schukkink, R., Dircks, M., Adriaanse, H., Malek, L., Sooknanan, R., and Lens, P. (1991) NASBA isothermal enzymatic in vitro nucleic acid amplification optimized for the diagnosis of HIV-1 infection. *J. Virol. Methods* **35**, 273–286
5. Ishiguro, T., Saitoh, J., Horie, R., Hayashi, T., Ishizuka, T., Tsuchiya, S., Yasukawa, K., Kido, T., Nakaguchi, Y., Nishibuchi, M., and Ueda, K. (2003) Intercalation activating fluorescence DNA probe and its application to homogeneous quantification of a target sequence by isothermal sequence amplification in a closed vessel. *Anal. Biochem.* **314**, 77–86
6. Roberts, J.D., Bebenek, K., and Kunkel, T.A. (1988) The accuracy of reverse transcriptase from HIV-1. *Science* **242**, 1171–1173
7. DeStefano, J.J., Buiser, R.G., Mallaber, L.M., Myers, T.W., Bambara, R.A., and Fay, P.J. (1991) Polymerization and RNase H activities of reverse transcriptases from avian myeloblastosis, human immunodeficiency, and Moloney murine leukemia viruses are functionally uncoupled. *J. Biol. Chem.* **266**, 7423–7431
8. Tanase, N., Roth, M., and Goff, S.P. (1985) Expression of enzymatically active reverse transcriptase in *Escherichia coli*. *Proc. Natl. Acad. Sci. USA* **82**, 4944–4948
9. Roth, M.J., Tanese, N., and Goff, S.P. (1985) Purification and characterization of murine retroviral reverse transcriptase expressed in *Escherichia coli*. *J. Biol. Chem.* **260**, 9326–9335
10. Kotewicz, M.L., D'Alessio, J.M., Driftmier, K.M., Blodqett, K.P., and Gerard, G.F. (1985) Cloning and overexpression of Moloney murine leukemia virus reverse transcriptase in *Escherichia coli*. *Gene* **35**, 249–258
11. Soltis, D.A. and Skalka, A.M. (1988) The α and β chains of avian retrovirus reverse transcriptase independently expressed in *Escherichia coli*: characterization of enzymatic activities. *Proc. Natl. Acad. Sci. USA* **85**, 3372–3376
12. Werner, S. and Wöhrl, B.M. (1999) Soluble Rous sarcoma virus reverse transcriptase α, αβ, and β purified from insect cells are processive DNA polymerases that lack an RNaseH 3′→5′ directed processing activity. *J. Biol. Chem.* **274**, 26329–26336
13. Georgiadis, M.M., Jessen, S.M., Ogata, C.M., Telesnitsky, A., Goff, S.P., and Hendrickson, W.A. (1995) Mechanistic implications from the structure of a catalytic fragment of Moloney murine leukemia virus reverse transcriptase. *Structure* **3**, 879–892
14. Das, D. and Georgiadis, M.M. (2004) The crystal structure of the monomeric reverse transcriptase from Moloney murine leukemia virus. *Structure* **12**, 819–829
15. Lim, D., Gregorio, G.G., Bingman, C., Martinez-Hackert, E., Hendrickson, W.A., and Goff, S.P. (2006) Crystal structure of the Moloney murine leukemia virus RNase H domain. *J. Virol.* **80**, 8379–8389
16. Kotewicz, M.L., Sampson, C.M., D'Alessio, J.M., and Gerard, G.F. (1988) Isolation of cloned Moloney murine leukemia virus reverse transcriptase lacking ribonuclease H activity. *Nucleic Acids Res.* **16**, 265–277
17. Gerard, G.F., Schmidt, B.J., Kotewicz, M.L., and Campbell, J.H. (1992) cDNA synthesis by Moloney murine leukemia virus RNase H-minus reverse transcriptase possessing full DNA polymerase activity. *Focus* **14**, 91–93
18. Masuda, N., Yasukawa, K., Isawa, Y., Horie, R., Saitoh, J., Ishiguro, T., Nakaguchi, Y., Nishibuchi, M., and Hayashi, T. (2004) Rapid detection of *tdh* and *trh* mRNAs of *Vibrio parahaemolyticus* by the transcription-reverse transcription concerted (TRC) method. *J. Biosci. Bioeng.* **98**, 236–243
19. Takakura, S., Tsuchiya, S., Isawa, Y., Yasukawa, K., Hayashi, T., Tomita, M., Suzuki, K., Hasegawa, T., Tagami, T., Kurashima, A., and Ichiyama, S. (2005) Rapid detection of *Mycobacterium tuberculosis* in respiratory samples by transcription-reverse transcription concerted reaction with an automated system. *J. Clin. Microbiol.* **43**, 5435–5439
20. Gerard, G.F. (1998) Reverse transcriptase: a historical perspective. *Focus* **20**, 65–67
21. Bradford, M.M. (1976) A rapid and sensitive method for the quantitation of microgram quantities of protein utilizing the principle of protein-dye binding. *Anal. Biochem.* **72**, 248–254
22. Laemmli, U.K. (1970) Cleavage of structural proteins during the assembly of the head of bacteriophage T4. *Nature* **227**, 680–685
23. Sakoda, M. and Hiromi, K. (1976) Determination of the best-fit values of kinetic parameters of the Michaelis-Menten equation by the method of least squares with Taylor expansion. *J. Biochem.* **80**, 547–555
24. Segel, I.H. (1975) *Enzyme kinetics,* pp. 926–942, John Wiley and Sons, New York
25. Gerard, G.F., Potter, R.J., Smith, M.D., Rosenthal, K., Dhariwal, G., Lee, J., and Chatterjee, D.K. (2002) The role of template-primer in protection of reverse transcriptase from thermal inactivation. *Nucleic Acids Res.* **30**, 3118–3129
26. Pace, C.N. and McGrath, T. (1980) Substrate stabilization of lysozyme to thermal and guanidine hydrochloride denaturation. *J. Biol. Chem.* **255**, 3862–3865
27. Beard, W.A. and Wilson, S.H. (1993) Kinetic analysis of template–primer interactions with recombinant forms of HIV-1 reverse transcriptase. *Biochemistry* **32**, 9745–9753
28. Inouye, K., Tanaka, H., and Oneda, H. (2000) States of tryptophyl residues and stability of recombinant human metalloproteinase 7 (matrilysin) as examined by fluorescence. *J. Biochem.* **128**, 363–369
29. Inouye, K., Osaki, A., and Tonomura, B. (1994) Dissociation of dimer of bovine erythrocyte Cu,Zn-superoxide dismutase and activity of the monomer subunit: effects of urea, temperature, and enzyme concentration. *J. Biochem.* **115**, 507–515
30. Lee, S., Mouri, Y., Minoda, M., Oneda, H., and Inouye, K. (2006) Comparison of the wild-type α-amylase and its variant enzymes in *Bacillus amyloliquefaciens* in activity and thermal stability, and insights into engineering the thermal stability of *Bacillus* α-amylase. *J. Biochem.* **139**, 1007–1015

31. Oneda, H., Lee, S., and Inouye, K. (2004) Inhibitory effect of 0.19 α-amylase inhibitor from wheat kernel on activity of porcine pancreas α-amylase and its thermal stability. *J. Biochem.* **135**, 421–427
32. Lee, S., Oneda, H., Minoda, M., Tanaka, A., and Inouye, K. (2006) Comparison of starch hydrolysis activity and thermal stability of two *Bacillus licheniformis* α-amylase and insights into engineering α-amylase variants active under acidic conditions. *J. Biochem.* **139**, 997–1005
33. Yutani, K., Ogasahara, K., Tsujita, T., and Sugino, Y. (1987) Dependence of conformational stability on hydrophobicity of the amino acid residue in a series of variant proteins substituted at a unique position of tryptophan synthase α subunit. *Proc. Natl. Acad. Sci. USA* **84**, 4441–4444
34. Shoichet, B.K., Baase, W.A., Kuroki, R., and Matthews, B.W. (1985) A relationship between protein stability and protein function. *Proc. Natl. Acad. Sci. USA* **92**, 452–456
35. Yasukawa, K. and Inouye, K. (2007) Improving the activity and stability of thermolysin by site-directed mutagenesis. *Biochim. Biophys. Acta* **1774**, 1281–1288
36. Mansfeld, J., Vriend, G., Dijkstra, B.W., Veltman, O.R., van den Burg, B., Venema, G., Ulbrich-Hofmann, R., and Eijsink, V.G. (1997) Extreme stabilization of a thermolysin-like protease by an engineered disulfide bond. *J. Biol. Chem.* **272**, 11152–11156
37. Patel, P.H., Jacobo-Molina, A., Ding, J., Tantillo, C., Clark, A.D. Jr., Raag, R., Nanni, R.G., Hughes, S.H., and Arnold, E. (1995) Insights into DNA polymerization mechanisms from structure and function analysis of HIV-1 reverse transcriptase. *Biochemistry* **34**, 5351–5363
38. Ding, J., Das, K., Hsiou, Y., Sarafianos, S.G., Clark, A.D. Jr., Jacobo-Molina, A., Tantillo, C., Hughes, S.H., and Arnold, E. (1998) Structure and functional implications of the polymerase active site region in a complex of HIV-1 RT with a double-stranded DNA template-primer and an antibody Fab fragment at 2.8 Å resolution. *J. Mol. Biol.* **284**, 1095–1111
39. Inouye, K., Izawa, S., Satio, A., and Tonomura, B. (1995) Effects of alcohols on the hydrolysis of colominic acid catalyzed by *Streptococcus* neuraminidase. *J. Biochem.* **117**, 629–634
40. Hashida, Y. and Inouye, K. (2007) Molecular mechanism of the inhibitory effect of cobalt ion on thermolysin activity and the suppressive effect of calcium ion on the cobalt ion-dependent inactivation of thermolysin. *J. Biochem.* **141**, 879–888
41. Hashida, Y. and Inouye, K. (2007) Kinetic analysis of the activation-and-inhibition dual effects of cobalt ion on thermolysin activity. *J. Biochem.* **141**, 843–853
42. Parnaik, V.K. and Das, M.R. (1983) A higher affinity of AMV reverse transripase for template-primers correlates with a lower rate of DNA synthesis. *FEBS Lett.* **161**, 145–148
43. Chowdhury, K., Kaushik, N., Pandey, V.N., and Modak, M.J. (1996) Elucidation of the role of Arg 110 of murine leukemia virus reverse transcriptase in the catalytic mechanism: biochemical characterization of its mutant enzymes. *Biochemistry* **35**, 16610–16620
44. Shi, Q., Singh, K., Srivastava, A., Kaushik, N., and Modak, M.J. (2002) Lysine 152 of MuLV reverse transcriptase is required for the integrity of the active site. *Biochemistry* **41**, 14831–14842
45. Whiting, S.H. and Champoux, J.J. (1998) Properties of strand displacement synthesis by Moloney murine leukemia virus reverse transcriptase: mechanistic implications. *J. Mol. Biol.* **278**, 559–577
46. Uneo, A. and Ishihama, A. (1982) Reverse transcriptase associated with avian sarcoma-leukosis viruses. II. Comparison of subunit structure and catalytic properties. *J. Biochem.* **91**, 323–330